13th Australasian Fluid Mechanics Conference
Monash University, Melbourne, Australia
13-18 December 1998

LABORATORY MODELLING OF FUMIGATION IN THE ATMOSPHERIC CONVECTIVE BOUNDARY LAYER

Mark F. HIBBERD[1]

CSIRO Atmospheric Research
Private Bag 1, Aspendale 3195, AUSTRALIA

ABSTRACT

Fumigation is an air pollution phenomenon in which an elevated plume is entrained into a developing convective boundary layer (CBL) and then rapidly mixed to the ground. A laboratory convection tank has been used to model the process. Dispersion results in the form of crosswind-integrated concentrations for the whole field were obtained using a quantitative video digitisation technique. Maximum crosswind-integrated ground level concentrations (GLCs) were found to be only weakly dependent on the CBL growth rate, but including a parameterisation for the lateral diffusion showed that the centreline GLCs increase with increasing growth rate.

INTRODUCTION

Fumigation is an air pollution phenomenon in which an elevated plume released into a stable air flow aloft is entrained into a developing CBL and rapidly mixed to the ground by the strong convective turbulence (e.g. Venkatram, 1988). It is an important process because it can lead to significant ground level concentrations of pollutants many kilometres downwind from a stack with little pollution in the intervening region. Fumigation is common in coastal industrial regions in Australia, where sea-breeze flows often produce thermal internal boundary layers (e.g. Sawford *et al.*, 1998). Fumigation also occurs at inland industrial sites during the morning growth of the CBL due to the associated break-up of the nocturnal temperature inversion.

A full description of the process requires consideration of the plume dispersion in both the initial stable layer aloft and the unstable CBL as well as the rate at which the plume crosses the entrainment zone between these two regions.

A number of numerical models have been developed to describe fumigation, e.g. Misra (1980), Stunder *et al.* (1986), Venkatram (1988), Luhar and Britter (1990), and Luhar and Sawford (1995). While all of these models account for the initial diffusion in the stable layer, the dispersion within the CBL is usually simplified by assuming it to be instantaneous (plume material entering the top of the CBL is immediately detected at the ground) and/or uniform (zero vertical concentration gradient). Improvements in the modelling of CBL dispersion have led to the application of probability density function models to describe this part of the fumigation process (e.g. Luhar and Sawford, 1996).

However, the influence of the entrainment zone thickness on the rate at which plume material is entrained into the CBL has generally been neglected. Its importance in reducing maximum GLCs and in extending the duration of fumigation episodes was pointed out in the laboratory experiments of Deardorff and Willis (1982). Later investigations by Hibberd and Luhar (1996) quantified its effect over a wide range of CBL growth rates. This paper focuses on the laboratory modelling techniques used in these experiments and the scope for quantitative video digitisation techniques.

EXPERIMENTAL METHOD

A series of laboratory experiments was carried out in a 3.2 m long, 1.6 m wide and 0.8 m deep saline convection tank described by Hibberd and Sawford (1994). This tank is able to model the turbulence structure of the convective boundary layer and the entrainment zone characteristic of penetrative convection into an overlying stable layer. The tank operates as an inverted model of the atmospheric CBL with the surface buoyancy flux delivered into the top of the mixed layer as a salty solution through a porous membrane. Strong downdraughts of denser salty water that form at the top of the tank correspond to thermal updraughts of warm air in the atmosphere. The mixed layer is "capped" from below by an inversion and a stably stratified layer, into which the CBL grows by penetrative convection. The CBL growth rate is controlled by the surface buoyancy flux, B_0, and the buoyancy frequency of the stable layer, $N = [(g/\rho)(d\rho/dz)]^{1/2}$, where $d\rho/dz$ is the density gradient in the stable layer. These parameters were adjusted to obtain a range of CBL growth rates from $0.002\ w_*$ to $0.15\ w_*$, where $w_* = (B_0\ z_i)^{1/3}$ is the convective velocity scale, characteristic of the CBL turbulence, and z_i is the depth of the CBL.

The experiments were designed to simulate the break up of a nocturnal inversion, although it can be shown that the results are also applicable to shoreline fumigation using a simple time-distance transformation. A ribbon of plume material about 2 m long was laid down in the stable layer by releasing the fumigant from a 4 mm diameter horizontal nozzle which was towed through the tank at the start of the experiment. The fumigant was a

[1] E-mail: mark.hibberd@dar.csiro.au

saline solution with a density matching that of the stable layer at the release height and containing 5% blue food dye. It was located at a distance z_{i0} below the top of the tank (approximately 0.3 m). During an experiment, the initial growth of the CBL towards the plume causes gravity waves in the stable layer, visible as undulations in the unfumigated ribbon. Finally parts of the CBL break through the mean height of the plume causing significant amounts of fumigant to be mixed into the CBL. Other parts of the ribbon remain aloft to be engulfed at later times.

Video Analysis Technique

The fumigation episodes were recorded using a Pulnix TM-6CN monochrome video camera with the automatic gain control off to maintain consistent quantitative measurements and the gamma index (relating camera output voltage to incident light intensity) set to 1. The camera was located 5 m in front of the front wall of the tank with illumination provided by four evenly spaced 500 W floodlamps situated behind a sheet of translucent acrylic on the back wall of the tank. The aperture of the video camera lens was carefully adjusted with no dye present to avoid saturation of the video image to white but to maintain maximum dynamic range. A schematic representation of the imaging system is shown in Fig. 1. In this set-up, the camera recorded crosswind-integrated dye concentrations.

The video recordings were digitised to 8-bit accuracy and 508×564 pixel resolution using a Coreco Oculus MX frame grabber in a 486 PC. Video pixel locations were converted to real laboratory coordinates in the centre-plane of the tank using a calibration derived from regularly spaced marker dots on the front and back walls of the tank. The digitised images were compared with a mean background frame with no dye present, which was obtained by averaging ten images that were recorded before the fumigant was laid down. The normalised pixel intensities at each pixel location were calculated as

$$I = \left(i_{bkg} - i\right)/i_{bkg} \qquad (1)$$

where i_{bkg} is the pixel intensity in the background frame and i is the pixel intensity of the analysed image (255=white, 0=black). These values of I were converted to concentrations using the calibration curve shown in Fig. 2. This was obtained using the same video set-up as

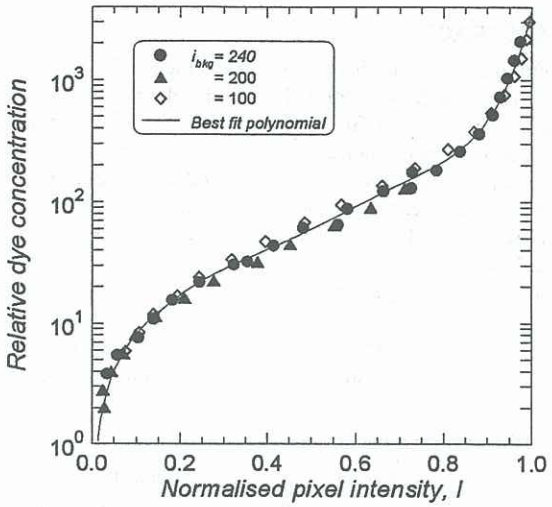

Figure 2. Calibration curve of dye concentration versus normalised pixel intensity.

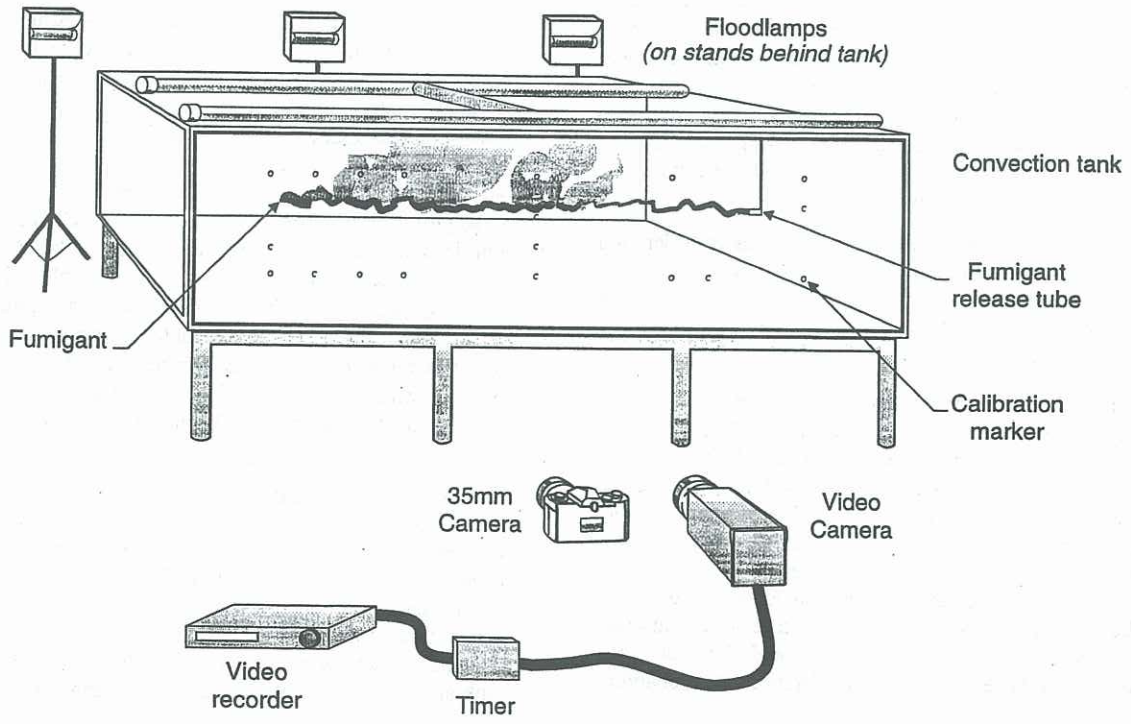

Figure 1. Schematic diagram of the experimental set-up.

in Fig. 1 but with a geometric progression of accurately known dye concentrations in a small 25 l tank. The normalisation using Eq. (1) produced overlap of the calibration data obtained with various values of c_{bkg}. For $I \leq 0.2$, the relation is linear, whereas in the range $0.2 < I < 0.8$, the log-linear plot of Fig. 2 shows that the relationship is exponential. In practice, for $I > 0.2$, a fifth order polynomial was used to describe the calibration curve.

For each image (at ~4 s timesteps), the concentrations at each pixel were averaged according to their vertical locations in bins 0.05 z_{i0} high and covering a horizontal region extending most of the horizontal extent of the initial ribbon. There were typically 2000 values per bin. Negative concentrations at individual pixels, arising from noise in the video and frame grabbing systems (± 2 grey levels), were carried over into the averaging to avoid thresholding errors. Averaging the large number of samples per bin provided reliable estimates of concentrations with a resolution equivalent to 0.5 grey level units or 0.02 dimensionless concentration units.

The dimensionless crosswind-integrated concentration used here is defined as

$$\overline{C}^{y}(Z,T) = \frac{z_{i0}\overline{c}^{y}}{Q_f} = \frac{z_{i0}}{Q_f}\frac{1}{l_r}\int_0^{l_r}\int_{-d/2}^{d/2}\overline{c}(l,y,z,t)\,\mathrm{d}y\,\mathrm{d}l \quad (2)$$

where $\overline{c}$ is the dimensional local, $\overline{c}^{y}(z,t)$ the mean dimensional crosswind-integrated concentration averaged over the ribbon length l_r, y the dimensional crosswind (lateral) coordinate, d the width of the tank, l the coordinate along the ribbon, and Q_f the source strength of the fumigant ribbon, which in convectional terms is equivalent to Q/U where Q is the flux (mass per unit time) released by a point source into a wind with mean speed U.

The initial fumigant height z_{i0} and the convective timescale $t_* = z_{i0}/w_*$ are used as scaling parameters for non-dimensionalising vertical height $Z=z/z_{i0}$ and elapsed times $T=(t - t_s)/t_*$, where t_s is the time at which fumigation starts.

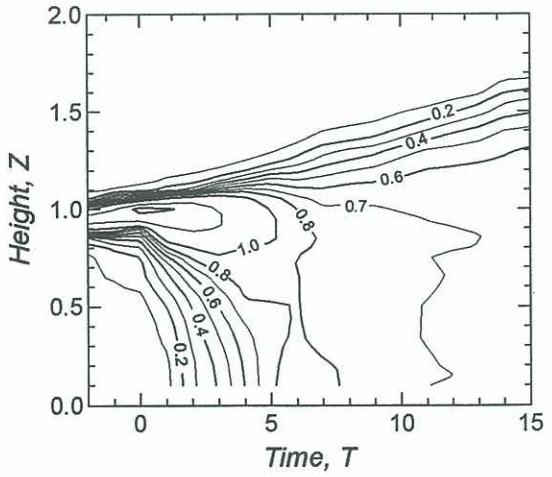

Figure 3. Contours of crosswind-integrated concentration $\overline{C}^{y}(Z,T)$ for CBL growth rate of 0.038 w_*.

The vertical concentration profiles at each time were combined to form a contour plot of $\overline{C}^{y}(Z,T)$. Fig. 3 shows an example for a CBL growth rate of 0.038 w_*. A final correction to the concentrations was applied by imposing the condition that the mass of dye within the analysis region be conserved as fumigation proceeded:

$$\int_0^{\infty}\overline{C}^{y}\,\mathrm{d}Z = 1. \quad (3)$$

RESULTS

Concentrations below about 0.1 z_{i0} were not able to be measured because of obstruction by towing cables. However, Fig. 3 shows that the concentration gradients in the lower part of the CBL were generally weak. Thus the measurements at 0.2 z_{i0} in Fig. 4 closely approximate ground level concentrations for the two experiments corresponding to the average in Fig. 3. The solid line represents the modified PDF model described by Hibberd and Luhar (1996) for these experimental conditions. There is close agreement between the data and the model predictions. The concentration $\overline{C}^{y}$ is seen to rise steadily to 0.8–0.9 at a time $T \approx 7$ and then decay slowly due to the increasing depth of the CBL.

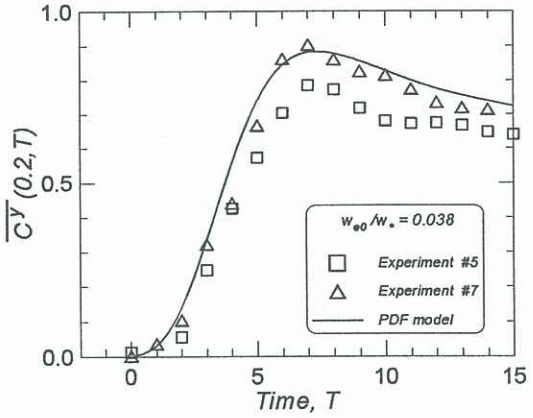

Figure 4. Near ground-level ($Z=0.2$) crosswind-integrated concentrations for the same conditions as shown in Fig. 3. The solid line is the PDF model described by Hibberd and Luhar (1996).

The influence of CBL growth rate on the crosswind-integrated concentrations near ground level is shown in Fig. 5 for growth rates from 0.014 w_* to 0.15 w_*. The PDF model predictions are shown rather than the data because the model matches the data closely and the scatter in the data would make it difficult to distinguish between the closely spaced curves. (The data and model are compared in detail by Hibberd and Luhar, 1996). At high growth rates, the peak is narrower and the maximum occurs earlier because the plume is entrained more rapidly. However, it can be seen that the peak values of the crosswind-integrated concentration remain approximately constant with changes in CBL growth rate.

Estimates of the centreline concentrations (C_{max}) can be derived from the crosswind-integrated concentrations by

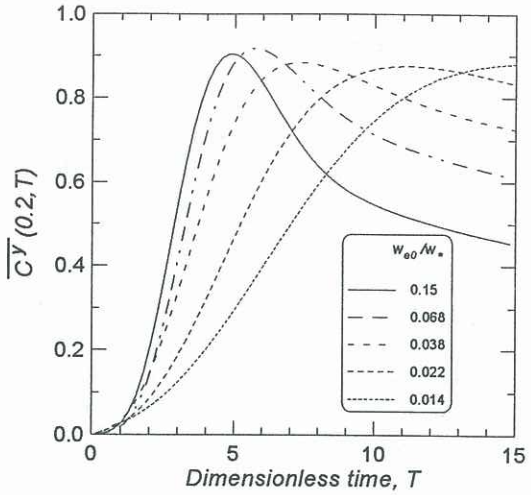

Figure 5. Influence of CBL growth rate on near ground-level crosswind-integrated concentrations.

assuming that the crosswind spread of the plume is Gaussian with a lateral dispersion coefficient σ_y:

$$C_{\max} = \overline{C}^y / \left(\sqrt{2\pi} \cdot \sigma_y\right). \quad (4)$$

Measurements of σ_y were not made for the experiments described here, but the results of Deardorff and Willis (1982) showed that for low growth rates (here 0.014 w_* and 0.022 w_*)

$$\sigma_y \approx 0.3T^{0.6} \quad (5)$$

whereas for higher growth rates

$$\sigma_y \approx 0.2T^{0.7}. \quad (6)$$

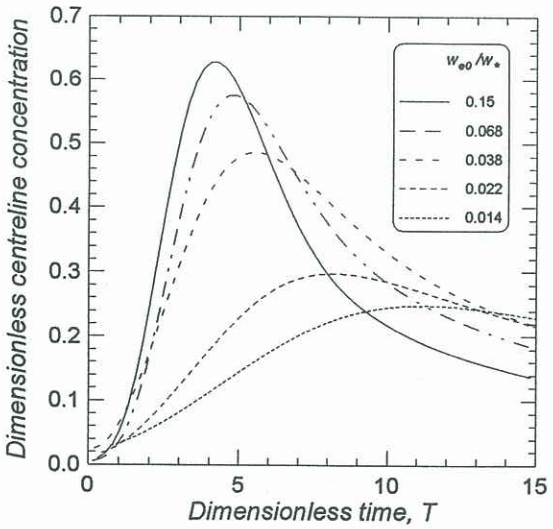

Figure 6. Influence of CBL growth rate on near ground-level ($Z=0.2$) centreline concentrations. Results estimated assuming a Gaussian lateral spread with diffusion coefficients given by Deardorff and Willis (1982).

Using these relations, the centreline concentrations shown in Fig. 6 were obtained from the results in Fig. 5. The peak centreline concentrations are seen to decrease strongly as the growth rate decreases with the peak also occurring at later times. Further experiments to measure the lateral dispersion coefficient are required to quantify this behaviour more accurately.

CONCLUSIONS

A laboratory convection tank has been used to study the influence of CBL growth rate on fumigation of a plume into an atmospheric CBL. A quantitative video analysis technique has been shown to be able to provide detailed dispersion data in the form of crosswind-integrated concentrations. A simple parameterisation of the lateral dispersion coefficient allows the average centreline concentrations to be calculated.

REFERENCES

DEARDORFF, J.W. and WILLIS, G.E., "Ground-level concentrations due to fumigation into an entraining mixed layer", *Atmos. Environ.* **16**, 1159–1170, 1982.

HIBBERD, M.F. and LUHAR, A.K., "A laboratory study and improved PDF model of fumigation into a growing convective boundary layer", *Atmos. Environ., 30, 3633–3649, 1996.*

HIBBERD, M.F. and SAWFORD, B.L., "A saline laboratory model of the planetary convective boundary layer for diffusion studies", *Boundary-Layer Met.* **67**, 229–250, 1994.

LUHAR, A.K. and BRITTER, R.E., "An application of Lagrangian stochastic modelling to dispersion during shoreline fumigation", *Atmos. Environ.* **24A**, 871–881, 1990.

LUHAR, A.K. and SAWFORD, B.L., "Lagrangian stochastic modelling of the coastal fumigation phenomenon", *J. Appl. Met.*, **34**, 2259–2277, 1995.

LUHAR, A.K. and SAWFORD, B.L., "An examination of existing shoreline fumigation models and formulation of an improved model", *Atmos. Environ.* **30**, 609–620, 1996.

MISRA, P.K., "Dispersion from tall stacks into a shoreline environment", *Atmos. Environ.* **14**, 397–400, 1980.

SAWFORD, B.L., LUHAR, A.K., HACKER, J.M., YOUNG, S.A., NOONAN, J.A., CARRAS, J.N., WILLIAMS, D.J. and RAYNER, K.N., "The Kwinana coastal fumigation study – I: Program overview, experimental design and selected results", *Boundary-Layer Met.* (in press) 1998.

STUNDER, M.J., SETHURAMAN, S., MISRA, P.K. and SAHOTA, H., "Downwind non-uniform mixing in shoreline fumigation processes", *Boundary-Layer Met.*, **34**, 177–184, 1986.

VENKATRAM, A., "Topics in applied dipsersion modelling", in: *Lectures on Air Pollution Modeling*, A Venkatram and J.C. Wyngaard (eds) Amer. Meteorol. Soc., Boston, 168-227, 1988.